JOURNAL OF CATALYSIS **168,** 60–69 (1997)
ARTICLE NO. CA971610

Toluene Hydrogenation Catalyzed by Tetrairidium Clusters Supported on γ-Al_2O_3

A. Zhao and B. C. Gates[1]

Department of Chemical Engineering and Materials Science, University of California, Davis, California 95616

Received June 21, 1996; revised January 2, 1997; accepted January 3, 1997

Supported clusters represented as Ir_4 on γ-Al_2O_3 were prepared by treatment of γ-Al_2O_3-supported $[Ir_4(CO)_{12}]$ in He at 300°C. The clusters were decarbonylated with near retention of the tetrahedral cluster frame, as indicated by extended X-ray absorption fine structure (EXAFS) spectra determining a first-shell Ir–Ir coordination number of 3.04 with a distance of 2.682 Å. X-ray absorption near-edge structure data characterizing the catalysts and Ir metal indicate the electron deficiency of the supported clusters, and the EXAFS data indicate an Ir–O distance of about 2.1 Å, which is consistent with bonding of cationic Ir in the clusters to oxygen of the support. The supported Ir_4 clusters were found to be catalytically active for the structure-insensitive toluene hydrogenation at temperatures in the range 60 to 100°C, with the activity being almost the same as that of Ir_6/γ-Al_2O_3 and an order of magnitude less than that of Ir aggregates of about 50 atoms each, on average, supported on γ-Al_2O_3. The Ir_4/γ-Al_2O_3 catalyst was stable in operation in a flow reactor, and, consistent with this observation, EXAFS results characterizing the used catalyst indicated that the cluster nuclearity was essentially unchanged after catalysis. The low activity of the supported Ir_4 clusters relative to that of metallic Ir particles indicates that the concept of structure insensitivity is no longer valid for clusters as small as Ir_4 on the metal oxide support.

INTRODUCTION

Supported metal clusters consisting of fewer than about 10 Pt atoms each (1–3) have recently found industrial application for selective dehydrocyclization of naphtha to give aromatics (4–6). In investigations of model-supported metal clusters comparable to those used in practice, metal carbonyl precursors, $[HIr_4(CO)_{11}]^-$ and $[Ir_6(CO)_{15}]^{2-}$, have been used to prepare nearly uniform supported clusters, approximated as Ir_4 (7, 8) and Ir_6 (9). The small clusters were reported to be markedly less active than conventional supported Ir particles for toluene hydrogenation; the results suggest that the concept of structure insensitivity in metal catalysis is no longer simply applicable when the metal entities are as small as four- or six-atom clusters (10–12). The limitation of the concept was suggested to be associated with the effect of the support as a ligand, which becomes maximized for the smallest clusters.

The availability of samples consisting of supported clusters to the near exclusion of other metal structures opens up the opportunity to determine how the catalytic properties depend on the nature of the metal, the cluster size, and the support. In the following, we report the synthesis, structural characterization, and catalytic performance of samples consisting predominantly of Ir_4/γ-Al_2O_3, providing the basis for a comparison of this catalyst with Ir_6/γ-Al_2O_3. Another goal of the work was to document the differences between these small clusters and Ir aggregates; this work constitutes one step toward meeting the larger goals of elucidating how cluster size and structure, metal–support interactions, and electronic (ligand) effects influence the catalytic properties of small, well-defined metal clusters.

EXPERIMENTAL METHODS

Materials

$[Ir_4(CO)_{12}]$ (98%, Strem) and Ir powder (2N8, Strem) were used as received. γ-Al_2O_3 (Aluminum Oxide C, Degussa) was made into a paste by adding deionized water, followed by drying overnight at 120°C. It was then ground and evacuated at 25°C overnight. The resultant γ-Al_2O_3 support was stored under N_2 in a Braun MB-150M glove box. *n*-Pentane (98%, Aldrich) was dried by refluxing over sodium benzophenone ketyl under N_2 and degassed. Toluene (99.7%, J. T. Baker) was degassed by sparging of N_2 (99.997%, Liquid Carbonic) for 2 h before use. He (99.995%) was supplied by Liquid Carbonic and passed through traps containing particles of Cu_2O and zeolite 4A to remove traces of O_2 and moisture. H_2 with a purity of 99.99% was generated by a Balston H_2 generator (Type 75-33) and passed through the same traps used for He.

Preparation of Supported Ir Catalysts

The catalyst precursor, $[Ir_4(CO)_{12}]$ supported on γ-Al_2O_3, was prepared by slurrying $[Ir_4(CO)_{12}]$ and γ-Al_2O_3

[1] To whom correspondence should be addressed.

0021-9517/97 $25.00

in freshly distilled *n*-pentane in a Schlenk flask under N_2. The mixture was stirred under N_2 for 12 h at room temperature and then dried by evacuation for 8 h at room temperature, leaving all of the Ir on the γ-Al_2O_3 surface. The powder was unloaded in the glove box and characterized by infrared spectroscopy (Bruker IFS-66v). The Ir content of the solid was 1 wt%.

The precursors were decarbonylated in He at 300°C for 2 h to form supported Ir clusters, or they were treated in flowing He at 400°C for 2 h, followed by treatment in flowing H_2 at 400°C for 2 h and then purging with He for 0.5 h at the same temperature to form Ir aggregates on γ-Al_2O_3.

Toluene Hydrogenation Catalysis

Toluene hydrogenation catalyzed by γ-Al_2O_3-supported tetrairidium clusters was carried out in a tubular flow reactor. The catalyst was pretreated *in situ* prior to the kinetics measurements. Typically, 40 mg of sample consisting of γ-Al_2O_3-supported $[Ir_4(CO)_{12}]$ was diluted with 400 mg of inert α-Al_2O_3 and loaded into the reactor to give a catalyst bed about 2 to 3 mm in depth. The supported iridium carbonyl precursors were decarbonylated in flowing He at 300°C for 2 h to form supported Ir clusters.

In a catalysis experiment, toluene was injected into the flow system at a constant rate by an Isco liquid metering pump (Model 260D), flowing to a vaporizer held at about 120°C. The reaction mixture consisted of H_2 and vaporized toluene, which passed at atmospheric pressure through the reactor at a total flow rate of 46 ml (NTP)/min. The reactor was mounted in an electrically heated and temperature-controlled Lindberg furnace. The effluent gas mixture was analyzed with an on-line Hewlett–Packard gas chromatograph (HP-5890 Series II) equipped with a DB-624 capillary column (J & W Scientific) and a flame ionization detector. The catalytic activity was measured in the once-through flow reactor under the following conditions: partial pressures, $P_{H_2} = 710$ Torr and $P_{toluene} = 50$ Torr; temperature = 60, 80, or 100°C.

After some of the experiments, the reactor was transferred to the glove box, and the catalyst, without coming in contact with air, was removed and stored for transfer to a synchrotron for X-ray absorption spectroscopy.

X-ray Absorption Spectroscopy

The X-ray absorption experiments were performed on beamline X-11A of the National Synchrotron Light Source (NSLS) at Brookhaven National Laboratory, Upton, Long Island, New York, and on beamline 2-3 of the Stanford Synchrotron Radiation Laboratory (SSRL) at the Stanford Linear Acceleration Center, Stanford, California. The storage ring at NSLS operated with an electron energy of 2.5 GeV, and that at SSRL, with an electron energy of 3 GeV. The beam current at NSLS was 140 to 240 mA, and that at SSRL was 40 to 100 mA.

Sample wafers for the transmission extended X-ray absorption fine-structure (EXAFS) spectroscopy experiments were prepared in glove boxes at the synchrotrons. The wafers were prepared as follows: Each powder sample was placed in a holder in the glove box. The holder was placed in a pressing die, and the sample was pressed into a self-supporting wafer. After pressing, the sample in the holder was mounted into a transmission EXAFS cell, described elsewhere (13), and sealed.

EXAFS data were recorded with the sample under vacuum and at approximately liquid nitrogen temperature. Higher harmonics in the X-ray beam were minimized by detuning the Si(111) double-crystal monochromator at NSLS by 15 to 20% or the Si(220) double-crystal monochromator at SSRL by 15 to 20% at the Ir L_{III} absorption edge (11215 eV).

Precautions were taken to allow transport of the samples from the University of California at Davis to the synchrotrons without air contamination. Each sample was placed inside double layers of glass vials, each individually sealed with a vial cap and Parafilm.

EXAFS DATA ANALYSIS

EXAFS Reference Data

The EXAFS data were analyzed with experimentally determined reference files obtained from EXAFS data for materials of known structure. The Ir–Ir and Ir–$O_{support}$ interactions were analyzed with phase shifts and backscattering amplitudes obtained from EXAFS data for Pt foil and $[Na_2Pt(OH)_6]$, respectively. The transferability of the phase shifts and backscattering amplitudes obtained from EXAFS data for Pt and Ir has been justified experimentally (14). The Ir–Al interaction was analyzed with phase shifts and backscattering amplitudes obtained from a theoretical Ir–Al EXAFS function calculated with the FEFF program (15) and adjusted to agree with the Ir–Al reference data obtained from IrAl alloy (7). The details of the preparation of the reference files are described elsewhere (7, 16), and the parameters used to extract these files from the EXAFS data are summarized in Table 1.

Analysis of EXAFS Data Characterizing Sample Formed by Decarbonylation of Supported Tetrairidium Carbonyl Clusters

The data analysis was performed with the Koningsberger difference file technique (19, 20) and the XDAP data analysis software (21) on the normalized EXAFS function characterizing the decarbonylated Ir clusters formed by thermal treatment of $[Ir_4(CO)_{12}]$ supported on γ-Al_2O_3. The analysis of the unweighted raw EXAFS data was done in *k* space (*k* is the wavevector), over the range $3.44 < k < 15.73$ Å^{-1},

TABLE 1

Structural Parameters Characterizing Reference Compounds and the Fourier Transform Ranges Used for Preparation of the Reference Files

Reference compound	Crystallographic data				Fourier transform[a]		
	Shell	N	r (Å)	Ref.	Δk (Å^{-1})	Δr (Å)	n
Pt foil	Pt–Pt	12	2.77	(17)	1.9–19.8	1.9–3.0	3
$Na_2Pt(OH)_6$	Pt–O	6	2.05	(18)	1.4–17.7	0.5–2.0	3
IrAl alloy	Ir–Al[b]	8	2.58	(7)	2.7–12.0[c]	0.98–2.98	3

[a] Notation: N, coordination number; Δk, limits of forward Fourier transformation (k is the wavevector); Δr, limits of shell isolation (r is the absorber–backscatterer distance); n, power of k used for Fourier transformation.

[b] After subtraction of Ir–Ir contribution: $N = 6$, $r = 2.98$ Å, Debye–Waller factor $\Delta\sigma^2 = -0.001$ Å^2, inner potential correction $\Delta E_0 = -3.3$ eV (7).

[c] A theoretical Ir–Al EXAFS function was calculated with the FEFF program (15) and adjusted to agree with the limited Ir–Al reference data obtained as described here for use of a larger interval in k space for fitting the Ir data (7).

as well as in r space (r is the distance from the absorber Ir atom) over the range $0 < r < 4$ Å. The Ir–Ir contribution was estimated by calculating an EXAFS function that agreed as closely as possible with the experimental results in the high-k range ($7.50 < k < 15.73$ Å^{-1}), as the metal–support contributions in this region are small. The EXAFS function calculated with the first-guess parameters was then subtracted from the overall EXAFS data, with the residual spectrum being expected to represent the Ir–support interactions. The difference file was estimated with two Ir–O contributions, Ir–O_s and Ir–O_l (where the subscripts represent short and long, respectively), as both short and long metal–support oxygen distances have been frequently observed for highly dispersed metal oxide-supported metals (22). More accurate parameter estimates were made by using the difference file technique, and the improved fits for the Ir–Ir, Ir–O_s, and Ir–O_l contributions were then added and compared with the raw data in both k space and r space.

The fit was not yet satisfactory. The Fourier transform of the residual spectrum showed an additional contribution at r equal to about 1.5 Å, which is tentatively suggested to be evidence of an interaction between Ir and Al of the support. The structural parameters characterizing the supposed Ir–Al contribution were determined by fitting the residual spectrum. The iteration was continued as stated above, until satisfactory overall agreement was achieved.

Analysis of EXAFS Data Characterizing Used Catalyst Formed by Decarbonylation of Supported Tetrairidium Carbonyl Clusters

The data analysis was performed on the normalized EXAFS function for the used catalyst, initially incorporating Ir_4/γ-Al_2O_3, in k space over the range $3.65 < k < 15.04$ Å^{-1}, as well as in r space over the range $0 < r < 4$ Å, by using the unweighted raw EXAFS data. The analysis procedure is the same as that stated above for the fresh catalyst.

Analysis of EXAFS Data Characterizing γ-Al_2O_3-Supported Ir Aggregates

The data analysis was performed on the normalized EXAFS function for the supported Ir aggregates (formed as described under Experimental Methods) in k space over the range $3.62 < k < 15.52$ Å^{-1}, as well as in r space over the range $0 < r < 5$ Å, by using unweighted raw EXAFS data. The analysis procedure is the same as that stated above for the fresh Ir_4/γ-Al_2O_3 catalyst except that the second- and third-shell Ir–Ir contributions were included in the fit.

Analysis of EXAFS Data Characterizing Ir Powder

The normalized EXAFS data characterizing Ir powder were Fourier filtered in r space in the range $0 < r < 3.5$ Å to isolate the first-shell Ir–Ir contribution from the higher-shell Ir–Ir contributions. The data analysis was performed in k space over the range $3.67 < k < 15.89$ Å^{-1}, as well as in r space over the range $0 < r < 3.5$ Å, by using the k^3-weighted isolated EXAFS function. Interactions between Ir and low-Z backscatterers were not evident, and therefore only the first-shell Ir–Ir contribution was included in the fit.

RESULTS

EXAFS Spectroscopy: Comparison of the Various Ir Samples

The decarbonylated Ir clusters formed *in situ* in the EXAFS cell via thermal treatment of γ-Al_2O_3-supported sample formed from $[Ir_4(CO)_{12}]$ in He at 300°C were characterized by EXAFS spectroscopy. The normalized EXAFS function for the decarbonylated clusters was obtained from the average of the X-ray absorption spectra from six scans, with the standard deviations in the EXAFS function being less than 0.001 over the whole range of k space; the raw EXAFS data show oscillations up to k equal to about 16 Å^{-1} (Fig. 1A).

The results of the EXAFS data analysis (Table 2) confirm the presence of Ir–Ir interactions and Ir-support interactions in the decarbonylated Ir clusters supported on γ-Al_2O_3. The latter include two Ir–O contributions and a small and questionable contribution attributed to Ir–Al. The structural parameters are summarized in Table 2. The number of parameters used to fit the data in the main-shell analysis is 16; the statistically justified number p, calculated from the Nyquist theorem (23) ($p = 2\Delta k \Delta r/\pi + 1$, where $\Delta k = 12.3$ Å^{-1} and $\Delta r = 4$ Å), is approximately 32. To show the goodness of fit, the comparisons of the raw EXAFS data and the fit in k space and in r space are shown in Figs. 1A

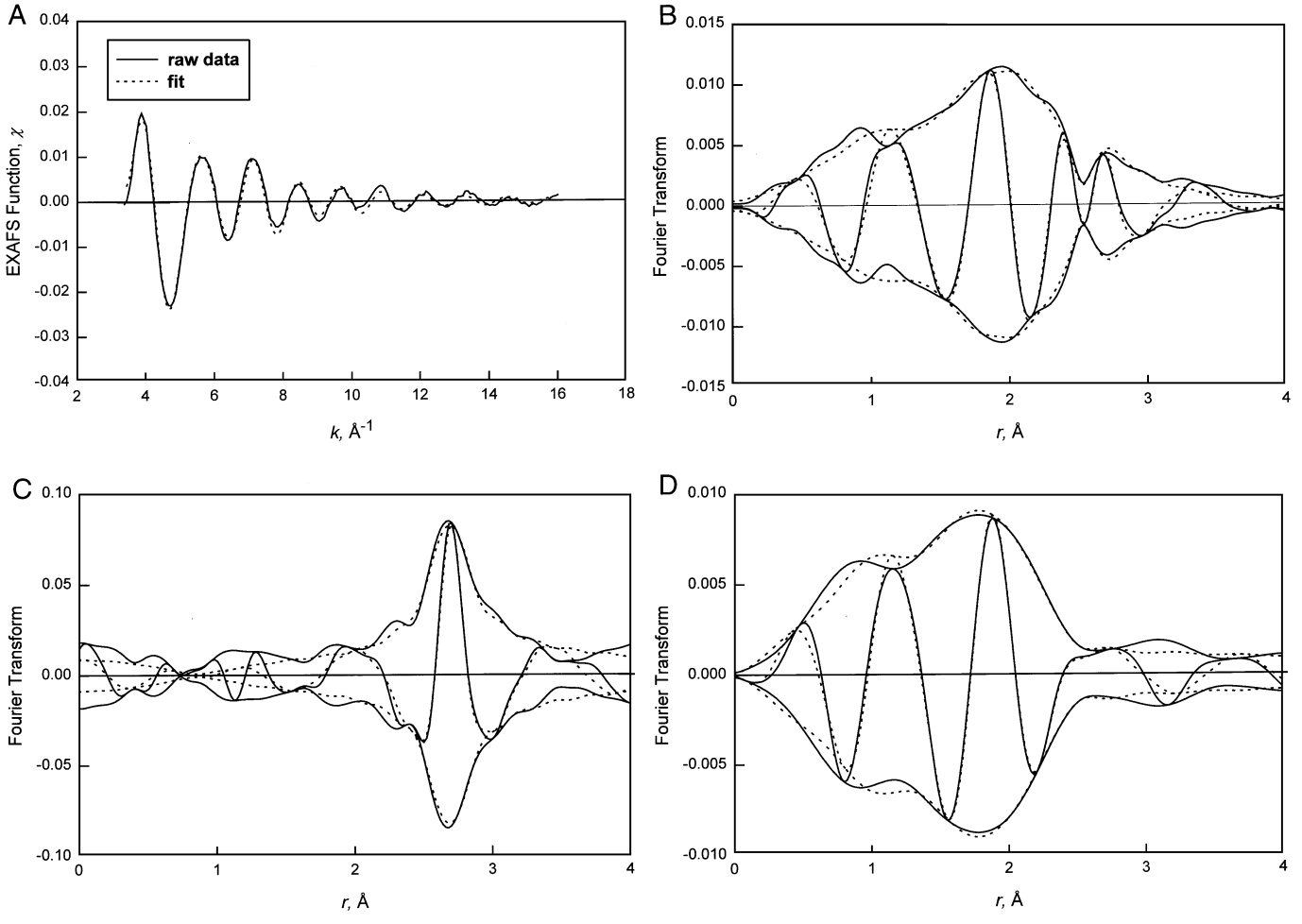

FIG. 1. Results of EXAFS analysis characterizing γ-Al_2O_3-supported Ir clusters formed by decarbonylation of γ-Al_2O_3-supported $[Ir_4(CO)_{12}]$ in He at 300°C for 2 h: (A) Raw EXAFS function (solid line) and sum of the calculated Ir–Ir + Ir–O_s + Ir–O_l + Ir–Al contributions (dashed line). (B) Imaginary part and magnitude of Fourier transform (unweighted, $\Delta k = 3.44$–15.73 Å^{-1}) of raw EXAFS function (solid line) and sum of the calculated Ir–Ir + Ir–O_s + Ir–O_l + Ir–Al contributions (dashed line). (C) Residual spectrum illustrating the Ir–Ir contribution; imaginary part and magnitude of Fourier transform (unweighted, $\Delta k = 3.44$–15.73 Å^{-1}) of raw EXAFS data minus calculated Ir–O_s + Ir–O_l + Ir–Al contributions (solid line) and calculated Ir–Ir contribution (dashed line). (D) Residual spectrum illustrating the contributions of metal–support interactions; imaginary part and magnitude of Fourier transform (unweighted, $\Delta k = 3.44$–10.0 Å^{-1}) of raw EXAFS data minus calculated Ir–Ir contribution (solid line) and calculated Ir–O_s + Ir–O_l + Ir–Al contributions (dashed line).

TABLE 2

EXAFS Results Characterizing the Ir Clusters Formed by Decarbonylation of $[Ir_4(CO)_{12}]$ on γ-Al_2O_3 in He at 300°C

Shell	Coordination number, N	Distance, r (Å)	$10^3 \times$ Debye–Waller factor, $\Delta\sigma^2$ (Å^2)	Inner potential correction, ΔE_0 (eV)	EXAFS reference
Ir–Ir	3.04	2.682	3.25	0.35	Pt–Pt
Ir–$O_{support}$					
Ir–O_s	1.04	2.098	3.08	1.68	Pt–O
Ir–O_l	1.19	2.630	−0.86	0.86	Pt–O
Ir–Al	0.86	1.538	13.78	20.03	Ir–Al

and B, respectively. The residual spectra giving evidence of the Ir–Ir and Ir–support contributions are shown in Figs. 1C and D, respectively.

The EXAFS results show a first-shell Ir–Ir coordination number of 3.04 with a bond distance of 2.682 Å, consistent with the presence of tetrahedral Ir_4. The decarbonylated Ir clusters are thus represented as Ir_4/γ-Al_2O_3, where it is implied that Ir_4 has a tetrahedral framework.

The results of the EXAFS data analysis for Ir aggregates supported on γ-Al_2O_3, formed after thermal treatment of γ-Al_2O_3-supported tetrairidium carbonyl clusters in He followed by H_2 at 400°C, indicate an average first-shell Ir–Ir coordination number of about 7 with a bond distance of 2.690 Å (Table 3). Thus, this catalyst consisted of small, and no doubt nonuniform, supported Ir aggregates of about

TABLE 3

First-Shell Ir–Ir Structure Parameters Determined by EXAFS Data Analysis for Ir Aggregates Supported on γ-Al_2O_3[a] and for Ir Powder

Sample	Shell	Coordination number, N	Distance, r (Å)	$10^3 \times$ Debye–Waller factor, $\Delta\sigma^2$ (Å^2)	Inner potential correction, ΔE_0 (eV)	EXAFS reference
Ir_{agg}/γ-Al_2O_3	Ir–Ir	7.20	2.690	3.67	−0.80	Pt–Pt
Ir powder	Ir–Ir	11.87	2.714	−0.19	−1.45	Pt–Pt

[a] The sample Ir_{agg}/γ-Al_2O_3 was formed by thermal treatment of [$Ir_4(CO)_{12}$] supported on γ-Al_2O_3 in He at 400°C for 2 h, followed by reduction in H_2 at 400°C for 2 h and then purging with He for 0.5 h.

50 atoms per aggregate, on average, with a dispersion of about 70% (24); the sample is represented as Ir_{agg}/γ-Al_2O_3.

The EXAFS results for Ir powder show a first-shell Ir–Ir coordination number of about 12 with a bond distance of 2.714 Å (Table 3), corresponding to the structural parameters of bulk Ir metal determined by X-ray diffraction (25). There is no indication of an Ir–O contribution in the EXAFS data. Thus, the Ir powder is almost equivalent to bulk Ir metal.

For a comparison of Ir_4/γ-Al_2O_3 with unsupported Ir metal and supported Ir clusters and aggregates with different nuclearities, Fourier transforms were calculated from the EXAFS data for the following: γ-Al_2O_3-supported Ir_4 (data from this work); γ-Al_2O_3-supported Ir_6 (12) (modeled as clusters of six atoms each on the basis of a first-shell Ir–Ir coordination number of 4); supported Ir aggregates with a first-shell Ir–Ir coordination number of about 7 (data from this work); and Ir powder (data from this work). All the Fourier transforms (Fig. 2A) were calculated with a k^3 weighting and were Pt–Pt phase and amplitude corrected.

It is evident that the magnitude of the Fourier transform at about 2.7 Å (the approximate first-shell Ir–Ir distance) increases with increasing cluster or particle nuclearity. The supported clusters designated as Ir_4/γ-Al_2O_3 and Ir_6/γ-Al_2O_3 are distinguishable from each other as well as from Ir_{agg}/γ-Al_2O_3, which is more representative of a conventional supported metal catalyst. The Ir metal powder is virtually infinite in nuclearity, as indicated by the prominent first, second, third, and fourth Ir–Ir shells in the Fourier transform and by the first-shell Ir–Ir coordination number of 12.

XANES Data: Comparison of the Various Ir Samples

Figure 2B shows the normalized Ir L_{III} X-ray absorption near-edge structure (XANES) data characterizing the samples mentioned above to provide a further comparison. Edge alignment was performed by setting the inflection point of each individual XANES spectrum to correspond to zero in the energy scale (26). The data show that the intensity of the white line increased with decreasing particle or cluster nuclearity.

Toluene Hydrogenation Catalyzed by Ir_4/γ-Al_2O_3

Toluene hydrogenation was carried out with the catalyst formed by decarbonylation of tetrairidium carbonyl clusters supported on γ-Al_2O_3 in He at 300°C for 2 h. The catalytic reaction was carried out in the differential mode, with conversions of toluene being less than 0.8%. The catalyst was stable for at least 10 h on stream; there was no indication of deactivation. The raw rate data correspond to steady-state operation and are represented in units of mol of toluene converted (g of catalyst · s)$^{-1}$, as shown in Fig. 3. The apparent activation energy obtained from the temperature dependence of the reaction rate was found to be 11.0 ± 0.3 kcal/mol, which is approximately the same as the value reported for toluene hydrogenation catalyzed by supported Pt and Pd catalysts consisting of metallic particles on metal oxide supports (27, 28).

These catalytic activity data characterizing toluene hydrogenation catalyzed by Ir_4/γ-Al_2O_3 are compared in Table 4 with those characterizing the reaction catalyzed by Ir_6/γ-Al_2O_3 and Ir_{agg}/γ-Al_2O_3. The catalytic activities are represented in Table 4 as turnover frequencies. The values for each catalyst were estimated per surface atom, and the supported Ir_4 and Ir_6 catalysts were assumed to be 100% dispersed on the support surface; the calculations were done ignoring the possibility that some Ir atoms were inaccessible because of interactions with the support. The data show that Ir_4/γ-Al_2O_3 has about the same activity as Ir_6/γ-Al_2O_3 for toluene hydrogenation, and it is an order of magnitude less active than Ir_{agg}/γ-Al_2O_3.

TABLE 4

Kinetics of Toluene Hydrogenation Catalyzed by γ-Al_2O_3-Supported Ir Catalysts at $P_{toluene} = 50$ Torr and $P_{H_2} = 710$ Torr

Catalyst	Temperature, (°C)	$10^3 \times$ catalytic activity (molecules of toluene/Ir atom · s)[a]
Ir_4/γ-Al_2O_3[b]	60	1.6
	80	3.5
	100	7.9
Ir_6/γ-Al_2O_3[c]	60	1.7
	80	3.8
	100	7.3
Ir_{agg}/γ-Al_2O_3[d]	60	13.9
	80	25.3
	100	50.4

[a] The activity is stated per surface Ir atom in the catalyst.

[b] Ir_4 was assumed to have 100% dispersion on the surface of γ-Al_2O_3 (data from this work).

[c] Ir_6 was assumed to have 100% dispersion on the surface of γ-Al_2O_3 (12).

[d] Ir aggregates were about 70% dispersed on the surface (12).

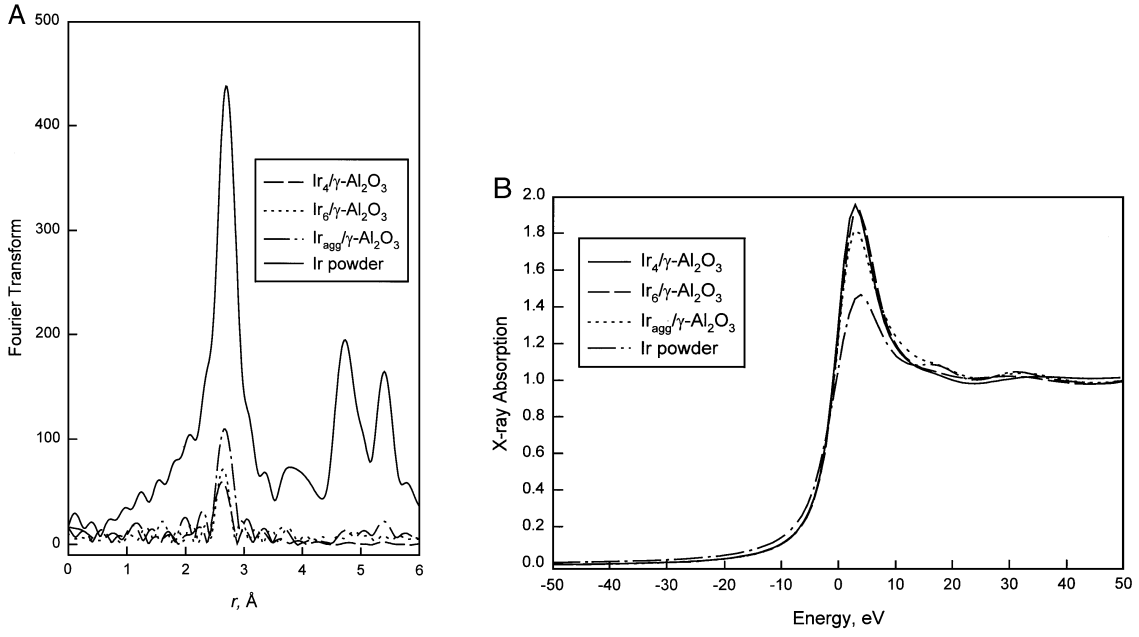

FIG. 2. Comparison of X-ray absorption data characterizing supported and unsupported Ir catalysts with different nuclearities: (A) Magnitude of Fourier transform (k^3-weighted, Pt–Pt phase and amplitude corrected) of EXAFS data characterizing Ir_4/γ-Al_2O_3 (dashed line, $\Delta k = 3.44$–15.73 Å^{-1}), Ir_6/γ-Al_2O_3 (dotted line, $\Delta k = 3.68$–16.26 Å^{-1}), Ir_{agg}/γ-Al_2O_3 (dashed–dotted line, $\Delta k = 3.62$–15.52 Å^{-1}), and Ir powder (solid line, $\Delta k = 3.67$–15.89 Å^{-1}). (B) XANES spectra of Ir_4/γ-Al_2O_3 (solid line), Ir_6/γ-Al_2O_3 (dashed line), Ir_{agg}/γ-Al_2O_3 (dotted line), and Ir powder (dashed–dotted line).

Characterization of Used Ir_4/γ-Al_2O_3 Catalyst by EXAFS Spectroscopy

A sample of the Ir_4/γ-Al_2O_3 catalyst that had been used in the flow reactor for 3 h on stream at 60°C with a H_2 partial pressure of 710 Torr and a toluene partial pressure of 50 Torr was characterized by EXAFS spectroscopy. The normalized EXAFS function was obtained from the average of the X-ray absorption spectra from six scans, with the standard deviation in the EXAFS function being less than 0.0005 over the whole range of k space; the raw EXAFS data show oscillations up to about $k = 16$ Å^{-1} (Fig. 4A).

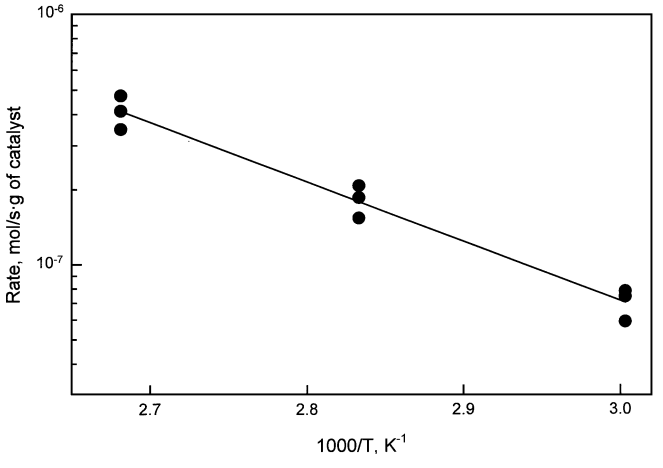

FIG. 3. Arrhenius plot for toluene hydrogenation catalyzed by γ-Al_2O_3-supported Ir_4 clusters. Reaction conditions: $P_{toluene} = 50$ Torr, $P_{H_2} = 710$ Torr; total feed flow rate: 46 ml (NTP)/min; catalyst mass: 40 mg, 1 wt% Ir.

The Fourier transforms of the raw EXAFS data characterizing the fresh and used Ir_4/γ-Al_2O_3 catalysts (Fig. 4B) are almost indistinguishable from each other, indicating that the catalyst was structurally stable. The normalized Ir L_{III} XANES spectra of the fresh and used Ir_4/γ-Al_2O_3 catalysts provide further evidence of this stability, as the two spectra are almost indistinguishable. Corresponding to these results, the first-shell Ir–Ir coordination number of the used catalyst was found to be 3.06 (Table 5), which is indistinguishable (within the expected experimental error of about ±20%) from the value characterizing the fresh Ir_4/γ-Al_2O_3 catalyst (Table 2). Thus, we conclude that, within our ability to determine the cluster nuclearity, the Ir_4/γ-Al_2O_3 catalyst remained unchanged during catalysis, which implies that the tetrahedral metal frame remained intact in the operation.

In addition to the Ir–Ir contribution to the EXAFS function, the data analysis also indicated contributions from Ir–O_s, Ir–O_l, and Ir–Al interactions. The structural parameters obtained from the data analysis are summarized in Table 5, and the comparison of the raw data and the fit in k space is shown in Fig. 4A. The number of parameters used to fit the data is 16; the statistically justified number, calculated from the Nyquist theorem ($\Delta k = 11.4$ Å^{-1}, $\Delta r = 4$ Å), is approximately 30.

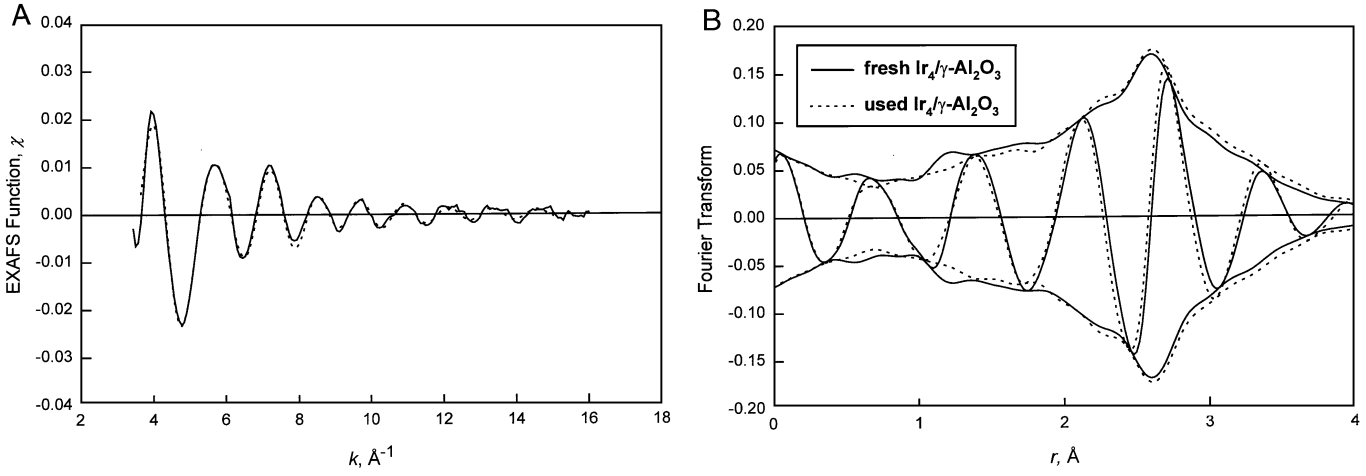

FIG. 4. X-ray absorption data characterizing the used Ir_4/γ-Al_2O_3 catalyst for toluene hydrogenation after being on stream for 3 h at 60°C and $P_{toluene} = 50$ Torr and $P_{H_2} = 710$ Torr: (A) Raw EXAFS function (solid line) and sum of the calculated Ir–Ir + Ir–O_s + Ir–O_l + Ir–Al contributions (dashed line). (B) Imaginary part and magnitude of Fourier transform (unweighted, $\Delta k = 3.65$–15.04 Å^{-1}, Pt–Pt phase and amplitude corrected) of raw EXAFS function of fresh Ir_4/γ-Al_2O_3 catalyst (solid line) and used Ir_4/γ-Al_2O_3 catalyst (dashed line).

DISCUSSION

Structurally Well-Defined Supported Tetrairidium Clusters

The raw EXAFS data characterizing the γ-Al_2O_3-supported Ir clusters formed by decarbonylation of $[Ir_4(CO)_{12}]$ on γ-Al_2O_3 are of high quality (Fig. 1A). The analysis indicates a first-shell Ir–Ir coordination number of 3.04, which is indistinguishable from 3 and consistent with the presence of tetrahedral Ir_4 clusters; evidently the clusters retained or nearly retained the tetrahedral metal frame of the precursor $[Ir_4(CO)_{12}]$ after removal of the carbonyl ligands. The absence of higher-shell Ir–Ir contributions in the Fourier transform is an indication of the lack of significant sintering of Ir to form larger aggregates or particles on the γ-Al_2O_3 surface. Thus, we infer that the clusters supported on γ-Al_2O_3 were nearly uniform Ir_4 tetrahedra, which were nearly molecular in character, being among the simplest and best defined supported metals.

The inference that Ir_4 clusters were formed by decarbonylation of γ-Al_2O_3-supported tetrairidium carbonyl clusters is in agreement with the report of Kawi *et al.* (29), who prepared the tetrairidium carbonyl precursor by surface-mediated synthesis from adsorbed $[Ir(CO)_2(acac)]$ on γ-Al_2O_3 in the presence of CO at room temperature, instead of by simple adsorption of $[Ir_4(CO)_{12}]$, as was done in this work. Furthermore, decarbonylation of supported tetrairidium carbonyl clusters with (near) retention of the metal frame has been reported to give Ir_4 on MgO (7, 8), NaY zeolite (30), and NaX zeolite (31), although the data characterizing the NaX zeolite are of relatively low quality and the structural inference less strong than for the other supports. Similarly, thermal treatment of hexairidium carbonyl clusters yielded clusters represented as Ir_6 on MgO (9), γ-Al_2O_3 (12), and NaY zeolite (32). These results demonstrate some generality of the methodology of preparing structurally well-defined Ir clusters by decarbonylation of the iridium carbonyl precursors, which have relatively stable metal frames.

The EXAFS data characterizing γ-Al_2O_3-supported tetrairidium clusters, hexairidium clusters (12), and Ir aggregates (with about 50 atoms per aggregate, on average) (Fig. 2A) show a pattern of increasing magnitude of the Fourier transform of the EXAFS data with increasing cluster or particle size. These data constitute a unique set of characterizations distinguishing a family of structurally well-defined supported and unsupported metals spanning nearly the largest attainable size range.

TABLE 5

EXAFS Results Characterizing Ir_4/γ-Al_2O_3 after Use as a Catalyst for Toluene Hydrogenation under the Following Conditions: $P_{toluene} = 50$ Torr, $P_{H_2} = 710$ Torr, Temperature = 60°C[a]

Shell	Coordination number, N	Distance, r (Å)	$10^3 \times$ Debye–Waller factor, $\Delta\sigma^2$ (Å^2)	Inner potential correction, ΔE_0 (eV)	EXAFS reference
Ir–Ir	3.06	2.674	3.07	−0.64	Pt–Pt
Ir–$O_{support}$					
Ir–O_s	0.84	2.092	0.14	−0.16	Pt–O
Ir–O_l	1.42	2.606	2.41	0.41	Pt–O
Ir–Al	0.90	1.535	14.78	23.45	Ir–Al

[a] The catalyst had been used for 3 h in the flow reactor.

A similar pattern was reported (7) for a family of MgO-supported Ir clusters; however, the samples prepared in the earlier work, which were formed by decarbonylation of tetrairidium carbonyl anions and hexairidium carbonyl anions on MgO, evidently consisted of mixtures of clusters, and the yields of tetrahedral Ir_4 and octahedral Ir_6 were about 50 and 25%, respectively. Thus, the preparations reported here for the γ-Al_2O_3 support were more successful in giving simple and well-defined clusters than those reported for the MgO support (7).

The comparison of the XANES data characterizing the various γ-Al_2O_3-supported and unsupported Ir samples at the Ir L_{III} absorption edge (Fig. 2B) provides further evidence distinguishing the samples. The increase in the white line intensity with decreasing particle or cluster nuclearity indicates that the transition probability of electrons being excited from core states (*s* or *p*) to empty *d* states is highest for the smallest clusters and least for the largest particles (33, 34); the data are consistent with the postulate that the smallest metal clusters are more electron deficient than the larger clusters and particles.

Retention of Structure of Supported Tetrairidium Clusters during Catalysis

The nearly exact match between the Fourier transforms of the EXAFS data characterizing the fresh and used Ir_4/γ-Al_2O_3 indicates that the clusters approximated as Ir_4 remained nearly intact during the catalysis. The results indicating that the first-shell Ir–Ir coordination number remained nearly unchanged (and nearly equal to 3, Tables 2 and 5) reinforce the inference that the tetrahedral clusters remained nearly intact during the catalytic operation. The good agreement of XANES spectra of the fresh and used Ir_4/γ-Al_2O_3 catalyst is additional evidence of the near lack of change in structure of the catalyst during operation; these data also indicate that the oxidation state of the Ir atoms in the clusters remained almost unchanged following the catalysis.

The data reported here add support to the evidence of stability of the family of structurally well-defined Ir clusters, at least under mild catalytic reaction conditions. For example, it has been reported on the basis of EXAFS experiments (10, 12) that Ir_4 on MgO, Ir_6 on MgO, Ir_6 on γ-Al_2O_3, and Ir_6 on NaY zeolite remained almost unchanged during toluene hydrogenation under the conditions used in this work. It was also reported (10) that Ir_4 on γ-Al_2O_3 remained intact after use for the same reaction, although the pretreatment of the γ-Al_2O_3 support was different from that described in this work; as a result, the extent of hydroxylation of the support (35) and consequently the catalytic performance were not the same for these samples of Ir_4/γ-Al_2O_3. Furthermore, Ir_4 on MgO has been found to be stable during use as a catalyst for propane hydrogenolysis at 200°C (36) and during use as a catalyst for cyclohexene hydrogenation at room temperature (11).

Catalytic Properties of Tetrairidium Clusters for Toluene Hydrogenation

The catalytic activity of Ir_4 supported on γ-Al_2O_3 for toluene hydrogenation is almost the same as that of Ir_6 on γ-Al_2O_3 (Table 4); however, each of these catalysts is an order of magnitude less active than the larger Ir aggregates on γ-Al_2O_3. Similarly, Ir_4 and Ir_6 supported on MgO were found to be less active than Ir aggregates on MgO (10). Thus the pattern emerging from all the available data is that the catalytic activities of metal oxide-supported Ir clusters, with nuclearities of about 4 or 6, are significantly less than those of supported Ir aggregates which are nearly metallic in character (10).

Hence the concept of structure insensitivity (37, 38) in metal catalysis, which has been shown to be valid for supported metals in the size range larger than about 10 Å, evidently does not extend straightforwardly to the domain of smaller clusters such as Ir_4 and Ir_6 on metal oxide supports (10, 12). Boudart and Sajkowski (39) reported that turnover frequencies for the structure-insensitive cyclohexene hydrogenation remained essentially unchanged for a family of alumina-supported Rh catalysts, with the smallest clusters having a nuclearity of roughly 12 atoms, on average, as determined by EXAFS data for the unused catalyst. Our results, taken together with those of Xiao *et al.* (40), who prepared Ir_4 on γ-Al_2O_3 and formed a family of samples with various average Ir aggregate and particle sizes by causing the metal to sinter to various degrees, suggest that a large change in turnover frequency is associated with changes in nuclearity in the range of fewer than roughly 100 atoms for toluene hydrogenation on γ-Al_2O_3-supported Ir catalysts.

We emphasize that these data do not necessarily indicate a simple metal cluster or particle size effect; the effects of the support are expected to be significant, as follows: As metal clusters on a metal oxide support become smaller, they are increasingly affected by metal–support interactions, which are expected to alter the electronic and thereby the catalytic properties of the metal. Evidence of the changing electronic properties is provided by the white line intensities (Fig. 2B), suggesting greater electron deficiency in the Ir atoms in the Ir_4 and Ir_6 clusters than in those in the larger Ir particles. Thus we infer that these small clusters are not comparable to bulk, metallic Ir, and the low catalytic activities are attributed, at least in part, to support effects that are in essence ligand effects. There are not yet sufficient data to separate cluster size and support (ligand) effects in supported metal cluster catalysis.

A comparison of the catalytic activity data characterizing Ir_4/γ-Al_2O_3, presented here, with the data reported by Xu *et al.* (10) for similar samples indicates that Ir_4 supported

on γ-Al_2O_3 is roughly three times as active as Ir_4 supported on MgO. Likewise, the comparison of published data for Ir_6 on γ-Al_2O_3 (12) and Ir_6 on MgO (10) indicates that the former is more active than the latter, by an order of magnitude. Thus the data are beginning to provide a basis for elucidation of the influence of the support on the activities of Ir clusters; however, we emphasize that there is likely an undetermined effect of support pretreatment conditions (affecting, e.g., the degree of hydroxylation), and more data are needed to establish these effects.

Nature of the Metal–Support Interface

The EXAFS data indicate two Ir–O contributions, at distances of about 2.1 and 2.6 Å. The shorter Ir–O distance is a bonding distance, consistent with the suggestion that the Ir bears a positive charge, but the longer distance is too long to be a bonding distance. The total Ir–O coordination number characterizing Ir_4 clusters on γ-Al_2O_3 was found to be about 2.2 (Table 2), whereas the value for Ir_6 clusters on γ-Al_2O_3 is about 1.5 (12). This comparison indicates the decreasing fraction of Ir atoms that reside at the metal–support interface as the cluster nuclearity increases. These results indicate that the maximum number of oxygen atoms associated with each Ir cluster (Ir_4 or Ir_6) was about 9.

Ir–Al contributions were also suggested on the basis of the EXAFS data analysis for both the Ir_4 and Ir_6 clusters, although these contributions are small and cannot be identified with confidence. The average Ir–Al coordination number characterizing Ir_4/γ-Al_2O_3 was found to be about 0.9, whereas the value for Ir_6/γ-Al_2O_3 was about 0.6; the results again point to a smaller fraction of Ir atoms at the metal–support interface for the larger Ir_6 clusters. These results indicate that the maximum number of Al cations that could be associated with each Ir cluster is approximately 3.6.

Contributions similar to the postulated Ir–Al contributions have been reported for Ir clusters supported on MgO (7) and Pt clusters supported in mordenite (41). Purnell *et al.* (42) postulated that clusters may reside preferentially at defect sites on MgO; likewise, Ir clusters may exist at defects on the γ-Al_2O_3 surface (12).

Therefore, on the one hand, the Ir–O and Ir–Al contributions provide a distinction between Ir_4 and Ir_6 clusters supported on γ-Al_2O_3; on the other hand, the result that equivalent numbers of O atoms interact with the Ir_4 and Ir_6 clusters suggests similar interface structures for Ir_4 and Ir_6; an equivalent statement pertains to the suggested Ir–Al interactions. Consequently, we present plausible models of the structures of the supported Ir clusters based on the EXAFS results (Fig. 5). At the metal–support interface, a triangular cluster face is postulated to interact with the support surface where Al atoms are exposed. The proposed model is simplified, and more data are needed to characterize the metal–support interface.

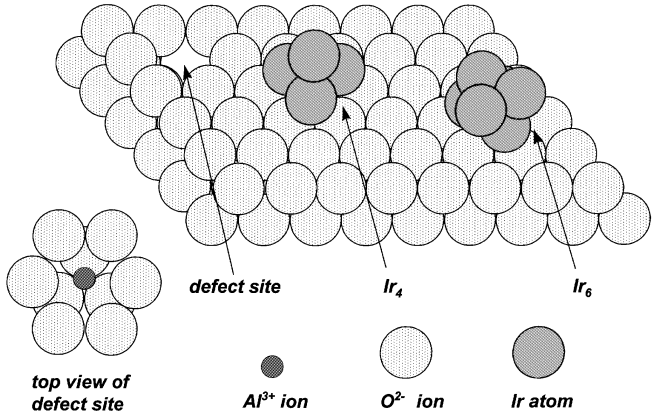

FIG. 5. Structural models of the Ir–γ-Al_2O_3 interface: Ir_4 and Ir_6 clusters on γ-Al_2O_3.

Ir–Ir Distances in the Supported Clusters and Aggregates

The EXAFS results showing the Ir–Ir distance in the supported clusters under vacuum before use (2.682 Å) and after use (2.674 Å) as a catalyst are indistinguishable within the expected experimental error of about ±1%. These distances are also indistinguishable from the value characterizing the supported Ir aggregates (2.690 Å), but they may be (barely) distinguishable from the value characterizing Ir metal powder (2.714 Å). This difference, if it is significant, might be attributed to the interactions of the supported clusters and aggregates with the support ligands, but the issues are unresolved.

Because the clusters supported on the γ-Al_2O_3 surface interact with O or OH groups on the support, it is plausible to regard them as coordinated to O or OH ligands and to bear positive charges to compensate for the negatively charged ligands, consistent with the XANES data discussed above. Presumably, the supported clusters are coordinatively unsaturated, with the open bonding sites providing positions for bonding of ligands. Effects of hydrogen ligands on the Ir–Ir distance in MgO-supported clusters modeled as Ir_4 are summarized elsewhere (43). Whether reactants bonded as ligands during catalysis modify the metal frame and the Ir–Ir distance of the supported clusters remains to be determined.

CONCLUSIONS

The CO ligands of tetrairidium carbonyl clusters supported on γ-Al_2O_3 were removed by treatment in He at 300°C, and the tetrahedral metal frame remained essentially intact, as indicated by EXAFS spectroscopy. Thus the decarbonylated clusters are represented as Ir_4/γ-Al_2O_3. These supported clusters are nearly uniform and nearly molecular in character, and the EXAFS and XANES data distinguish them clearly from Ir_6 on γ-Al_2O_3 and larger Ir

aggregates on γ-Al_2O_3. Ir_4/γ-Al_2O_3 catalyzes toluene hydrogenation at temperatures in the range 60 to 100°C; its catalytic activity is almost the same as that of Ir_6/γ-Al_2O_3 but an order of magnitude less than that of Ir aggregates (consisting of about 50 atoms each, on average) supported on γ-Al_2O_3. The catalyst was stable in operation in a flow reactor, and the EXAFS results confirm that the supported clusters approximated as Ir_4 remained intact during catalysis. As toluene hydrogenation is known to be a structure insensitive catalytic reaction, the results suggest that the concept of structure insensitivity does not extend to metal oxide-supported metal clusters as small as Ir_4 or Ir_6. The difference in catalytic activity between supported Ir_4 and Ir_6, on the one hand, and supported Ir aggregates, on the other hand, may be, at least in part, a consequence of the support's role in withdrawing electron density from the Ir clusters, as evidenced by XANES spectroscopy, rather than simply an effect of cluster size.

ACKNOWLEDGMENTS

This research was supported by the National Science Foundation (Grant CTS-9315340). We acknowledge beam time and the support of the U.S. Department of Energy, Division of Materials Sciences, under Contract DE-FG05-89ER45384, for its role in the operation and development of beam line X-11A at the National Synchrotron Light Source. The NSLS is supported by the Department of Energy, Division of Materials Sciences and Division of Chemical Sciences, under Contract DE-AC02-76CH00016. We are grateful to the staff of beam line X-11A for their assistance. We also acknowledge the Stanford Synchrotron Radiation Laboratory for access to beam time. The EXAFS data were analyzed with the XDAP software developed by Vaarkamp *et al.* (21)

REFERENCES

1. Vaarkamp, M., Grondelle, J. V., Miller, J. T., Sajkowski, D. J., Modica, F. S., Lane, G. S., Gates, B. C., and Koningsberger, D. C., *Catal. Lett.* **6**, 369 (1990).
2. Gates, B. C., *Chem. Rev.* **95**, 511 (1995).
3. (a) Vaarkamp, M., Modica, F. S., Miller, J. T., and Koningsberger, D. C., *J. Catal.* **144**, 611 (1993); (b) Meyers, B. L., Modica, F. S., Lane, G. S., Vaarkamp, M., and Koningsberger, D. C., *J. Catal.* **143**, 395 (1993).
4. *Oil Gas J.* **190**, 29 (1992).
5. Rotman, D., *Chem. Week* **150**, 8 (1992).
6. Hughes, T. R., Buss, W. C., Tamm, P. W., and Jacobson, R. L., *in* "New Developments in Zeolite Science and Technology" (Y. Murakami, A. Iijima, and J. W. Ward, Eds.), p. 725. Elsevier, Amsterdam, 1986.
7. van Zon, F. B. M., Maloney, S. D., Gates, B. C., and Koningsberger, D. C., *J. Am. Chem. Soc.* **115**, 10317 (1993).
8. Triantafillou, N. D., and Gates, B. C., *J. Phys. Chem.* **98**, 8431 (1994).
9. Maloney, S. D., Kelley, M. J., Koningsberger, D. C., and Gates, B. C., *J. Phys. Chem.* **95**, 9406 (1991).
10. Xu, Z., Xiao, F.-S., Purnell, S. K., Alexeev, O., Kawi, S., Deutsch, S. E., and Gates, B. C., *Nature (London)* **372**, 346 (1994).
11. Xu, Z., and Gates, B. C., *J. Catal.* **154**, 335 (1995).
12. Zhao, A., and Gates, B. C., *J. Am. Chem. Soc.* **118**, 2458 (1996).
13. Jentoft, R. E., Deutsch, S. E., and Gates, B. C., *Rev. Sci. Instrum.* **67**, 2111 (1996).
14. Duivenvoorden, F. B. M., Koningsberger, D. C., Uh, Y. S., and Gates, B. C., *J. Am. Chem. Soc.* **108**, 6254 (1986).
15. Lu, D., and Rehr, J. J., *J. Phys. (Paris) C8* **47**, 67 (1986).
16. van Zon, F. B. M., Ph.D. dissertation, Eindhoven University of Technology, Eindhoven, 1988.
17. Wyckoff, R. W. G. (Ed.), "Crystal Structures," 2nd ed., Vol. 1, p. 10. Wiley, New York, 1963.
18. Trömel, M., and Lupprich, E., *Z. Anorg. Chem.* **414**, 160 (1975).
19. van Zon, J. B. A. D., Koningsberger, D. C., van't Blik, H. F. J., and Sayers, D. E., *J. Chem. Phys.* **82**, 5742 (1985).
20. Kirlin, P. S., van Zon, F. B. M., Koningsberger, D. C., and Gates, B. C., *J. Phys. Chem.* **94**, 8439 (1990).
21. Vaarkamp, M., Linders, J. C., and Koningsberger, D. C., *Physica B* **209**, 159 (1995).
22. Koningsberger, D. C., and Gates, B. C., *Catal. Lett.* **14**, 271 (1992).
23. Crozier, E. D., Rehr, J. J., and Ingalls, R., *in* "X-ray Absorption: Principles, Applications, Techniques of EXAFS, SEXAFS, and XANES" (D. C. Koningsberger and R. Prins, Eds.), p. 395. Wiley, New York, 1988.
24. Kip, B. J., Duivenvoorden, F. B. M., Koningsberger, D. C., and Prins, R., *J. Catal.* **105**, 26 (1987).
25. Weast, W. C., and Astle, M. J., (Eds.), "Handbook of Chemistry and Physics," F-219. CRC Press, Boca Raton, FL, 1980.
26. Mansour, A. N., Cook, J. W., and Sayers, D. E., *J. Phys. Chem.* **88**, 2330 (1984).
27. Lin, S. D., and Vannice, M. A., *J. Catal.* **143**, 554 (1993).
28. Rahaman, M. V., and Vannice, M. A., *J. Catal.* **127**, 251 (1991).
29. Kawi, S., Chang, J.-R., and Gates, B. C., *J. Phys. Chem.* **97**, 5375 (1993).
30. Kawi, S., Chang, J.-R., and Gates, B. C., *J. Phys. Chem.* **97**, 10599 (1993).
31. Kawi, S., and Gates, B. C., *J. Phys. Chem.* **99**, 8824 (1995).
32. Kawi, S., Chang, J.-R., and Gates, B. C., *J. Am. Chem. Soc.* **115**, 4830 (1993).
33. Lytle, F. W., Wei, P. S. P., Greegor, R. B., Via, G. H., and Sinfelt, J. H., *J. Chem. Phys.* **70**, 4849 (1979).
34. Lytle, F. W., *J. Catal.* **43**, 376 (1976).
35. Knözinger, H., and Ratnasamy, P., *Catal. Rev. Sci. Eng.* **17**, 31 (1978).
36. Kawi, S., Chang, J.-R., and Gates, B. C., *J. Phys. Chem.* **98**, 12978 (1994).
37. Boudart, M., *J. Mol. Catal.* **30**, 27 (1985).
38. Boudart, M., and Djéga-Mariadassou, G., "Kinetics of Heterogeneous Catalytic Reactions." Princeton Univ. Press, Princeton, NJ, 1984.
39. Boudart, M., and Sajkowski, D. J., *Faraday Discuss. Chem. Soc.* **92**, 57 (1991).
40. Xiao, F.-S., Weber, W. A., Alexeev, O., and Gates, B. C., *in* "Proceedings of the 11th International Congress on Catalysis" (J. W. Hightower and W. N. Delgass, Eds.), Part B, p. 1135. Elsevier, Amsterdam, 1996.
41. Otten, M. K., Reifsnyder, S. N., and Lamb, H. H., *Physica B* **209**, 651 (1995).
42. Purnell, S. K., Xu, X., Goodman, D. W., and Gates, B. C., *J. Phys. Chem.* **98**, 4076 (1994).
43. Deutsch, S. E., Mestl, G., Knözinger, H., and Gates, B. C., *J. Phys. Chem.* **101**, 1374 (1997).